Effect of Nanosized Clay and TiO_2 on the Structure and Thermal Stability of Poly(aniline-co-o-toluidine)

J. Juliet Latha Jeyakumari[a], A. Yelilarasi[b,*] and R. Anbarasan[c]
[a]Department of Physics, PSN College, Tirunelveli, Tamil Nadu, India
[b]Department of Physics, KCET, Virudhunagar-626 001, Tamil Nadu, India
[c]Department of Polymer Technology, KCET, Virudhunagar-626 001, Tamil Nadu, India

(Received April 27, 2013; in final form September 21, 2013)

The present investigation is primarily focused on the study of effect of nanosized clay and TiO_2 on the structure and thermal properties of electrically conducting poly (aniline-co-o-toluidine)/nanocomposite system. These nanocomposites are synthesized by the *in situ* oxidative polymerization method with peroxy disulphate as a lone chemical initiator, HCl as an external dopant and clay and TiO_2 as a host material. The nanocomposites are characterized by analytical tools like Fourier transform infrared, Keithley instrument, thermal gravimetric analysis, and high resolution transmission electron microscopy.

DOI: 10.12693/APhysPolA.125.23
PACS: 39.30.+w

1. Introduction

Recently, the chemists are very much interested in synthesis and analysis of organic-inorganic host-guest matrix because of their novel properties. Meanwhile the synthetic polymer chemists are keen interested in the synthesis and characterizations of polymer-layered nanomaterials composite with boosted physical and chemical properties. In that series poly (aniline) (PANI), an electronic conducting polymer plays a vital role in the latest human being's luxurious life. For example, optical fiber based humidity sensor was made up by PANI copolymer [1]. Aniline-anthranilic acid copolymer film is being used as a pH sensor [2]. For such a super sensing activity, the structure of polymer is primarily important. Hence, many forces like nature of dopant, initiator, temperature and reaction time can alter the structure of polymer/copolymer. The structure of such a conducting polymer/copolymer can be nicely tuned with the aid of nanosized inorganic host materials. Recently, aniline copolymer intercalated meso structured MnO_2 composite was reported by Wang et al. [3]. Basavaraja and co-workers [4] studied the effect of Al_2O_3 on the structure of aniline-NIPAAm copolymer. PANI intercalated Au nanocomposite was prepared for NH_3 gas sensing [5]. Improved electro-rheological effect of PANI intercalated clay nanocomposite suspension was reported by Lim et al. [6]. Alcohol sensors made up by V_2O_5-PANI nanocomposite with high toughness has been reported in the literature [7]. PANI and its copolymers are made into nanocomposites with different inorganic host matrix [8–10]. The availability, eco-friendly, inexpensive, easy surface modification process and catalytic activity of clay and TiO_2 urged us to use clay and TiO_2 as a nanomaterial in the present investigation.

Moreover, this method is economically cheaper than the chemical method with more accuracy. FTIR spectrometer is a useful tool in various science and engineering fields, because of its high sensitivity or detectivity towards traces amount of sample, low noise to signal ratio and moreover this method is an easy and inexpensive one. FTIR spectroscopy is used in both qualitative [11–15] quantitative analysis [16–28]. For the first time, we are reporting here about the effect of clay and TiO_2 on the structure of aniline copolymer and the results are expressed.

2. Experimental

2.1. Materials

Aniline (ANI, M_1), o-toluidine (OT, M_2) were purchased from Merck, India and distilled under vacuum before use. Potassium peroxydisulphate (PDS), titanium oxide (TiO_2) (Ottokemi, India) and hydrochloric acid (Rea Chem, India) were used as received. Hectorite type Clay with Li^+ ion in the inner layer space was collected from our KCET campus and used after acid, base washing followed by washing with doubly distilled (DD) water. Thus, purified clay samples are dried and stored in a zipper bag. The clay details are indicated in our earlier publication [29].

2.2. Sample preparation method

Required quantity of ANI and OT solutions were taken in a polymer tube and de-aerated for 30 min. The copolymerization was initiated by the addition of calculated volumes of pre-aerated oxidizing agent such as PDS. The time of adding the oxidizing agent was taken as the starting time of the reaction. The reaction mixture was found

*corresponding author; e-mail: yeliloct1@gmail.com

to turn green in color and visible appearance of the polymer formation was noticed. After 2 h, air was blown into the polymer tube to freeze further reaction. The copolymerization was carried out at different reaction time and for different temperatures. Thus formed poly(ANI-co--OT) was filtered through already weighed G4 sintered crucible. The difference in weight gave the weight of copolymer formed. The same method was followed for the preparation of poly(ANI-co-OT)nanocomposites in the presence of different (weight% of clay and TiO_2).

2.3. Measurements

FTIR spectra of PANI samples were measured by the KBr pellet technique in the range of 4000–400/cm with Shimadzu 8400 S FTIR spectrophotometer instrument. The baseline correction was made carefully and the area of the peaks was determined using FTIR software. We know that PANI backbone is made up of benzenoid, quinonoid and semiquinonoid forms. The amount of formation of semiquinonoid form is negligible because it can be readily oxidized or reduced. Hence, we can write,

$$\text{Structure of PANI} = \%\ \text{amino form (benzenoid form)} + \%\ \text{imino form (quinonoid form)}. \quad (1)$$

Thermal gravimetric analysis (TGA) was performed under air purge at the heating rate of 10 °C/min by using SDT 2960 simultaneous TGA and differential scanning calorimetry (DSC), TA instruments. Conductivity was determined by standard four probe method. High resolution transmission electron microscopy (HRTEM) was recorded by using TEM 3010 Transmission Electron Microscopy instrument, a product of JEOL.

3. Results and discussion

3.1. FTIR study

Figure 1 showed the FTIR spectra of 1 to 5 wt% of clay loaded poly(ANI-co-OT) systems. The important peaks are characterized below. Spectrum showed many peaks among which we are very much interested in peaks appearing at 799, 1482, and 1563 cm^{-1} corresponding to the C–H out of plane bending vibration, benzenoid stretching, and quinonoid stretching, respectively. Peaks appearing at the lower wave number are corresponding to the metal oxide stretching of clay. Figure 2 showed the FTIR spectra of 1 to 5 wt% of TiO_2 loaded poly(ANI-co--OT) systems. Here also one can see the above-mentioned peaks, along with the 500 cm^{-1} confirming the presence of TiO_2.

3.2. Effect of time on R_p and FTIR-RI of PANI copolymers

Poly(ANI-co-OT)/clay nanocomposites were synthesized under different intervals of time. Variation in reaction time affected the R_p. While varying the reaction time from 3600 to 12600 s the other experimental conditions were kept constant. While increasing the time the R_p value was found to be decreased. This is due

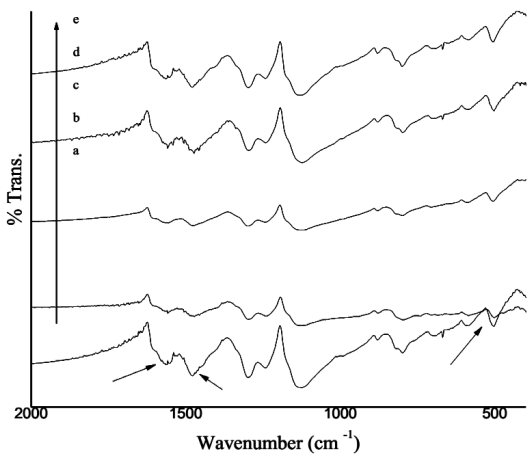

Fig. 1. FTIR spectrum of poly(ANI-co-OT) loaded with clay at (*a*) 1 wt%, (*b*) 2 wt%, (*c*) 3 wt%, (*d*) 4 wt%, (*e*) 5 wt%.

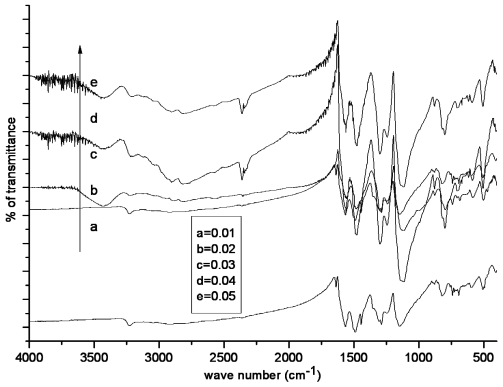

Fig. 2. FTIR spectrum of poly(ANI-co-MT) loaded with TiO_2 at (*a*) 1 wt%, (*b*) 2 wt%, (*c*) 3 wt%, (*d*) 4 wt%, (*e*) 5 wt%.

to the bulk number in the denominator of R_p equation. This is represented in Fig. 3a. Similarly, in the case of poly(ANI-co-OT)/TiO_2 the R_p value was decreased with increase in time (Fig. 3b). In comparison, the PANI-TiO_2 containing copolymer system produced higher R_p values than the copolymer clay system. Variation in reaction time affected the structure of copolymer, too. This is explained as follows: (1) Increase of reaction time leads to the possible interaction between monomer radical cations and free radicals with monomers. (2) Internal structural rearrangements.

3.3. Effect of [M] on R_p and FTIR-RI of PANI copolymers

The $[M_1/M_2]$ was varied between 0.40 and 1.60 while the other experimental conditions were kept constant. Here one can see that while increasing the [M], the R_p is increased simultaneously. This is due to the following reasons. (1) Availability of monomer radical cations for the chain growing process [23]. (2) Auto acceleration

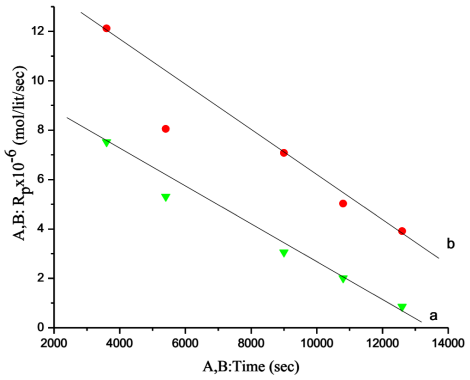

Fig. 3. Effect of time on R_p, (*a*) (ANI-co-OT)/clay, (*b*) poly(ANI-co-OT)/TiO_2, [ANI] = 0.125 M, [OT] = 0.125 M, [PDS] = 0.025 M, temperature = 45 °C, wt% of clay and TiO_2 = 3.

effect due to the surface of formed copolymer. (3) Active surface catalytic effect of nanosized clay and TiO_2. The molecular weight determination of copolymer chain by GPC method is under investigation in our lab. In order to find out the order of reaction $\log[M_1/M_2]$ vs. $\log R_p$ (Fig. 4a) was made.

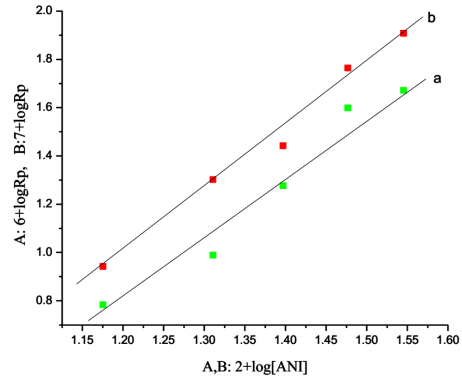

Fig. 4. Effect of $[M_1/M_2]$ on R_p, (*a*) poly(ANI-co-OT)/clay systems, (*b*) poly(ANI-co-OT)/TiO_2 system [PDS] = 0.025 M, time = 2 h, temperature = 45 °C, wt% of nanomaterial = 3.

The plot indicated a straight line with the slope value of 0.95. This indicates that copolymerization of ANI with OT in the presence of clay proceeds through 1.0 order of reaction with respect to $[M_1/M_2]$. The R_p can be written as follows: $R_p \propto [M_1/M_2]^{0.95}$. Similarly, in the case of poly(ANI-co-OT)/TiO_2, the R_p value increased with the [M]. In order to find out the order of reaction, the slope value was determined from the graph drawn between $\log[M_1/M_2]$ and $\log R_p$ as 0.98 (Fig. 4b). This confirmed the 1.0 order of reaction with respect to $[M_1/M_2]$. The R_p can be written as follows: $R_p \propto [M_1/M_2]^{0.98}$. On comparison, the TiO_2 containing copolymer nanocomposite system produced higher R_p values than the clay containing copolymer nanocomposite. The order of reaction indicated the uni-molecular termination reaction.

3.4. Effect of [PDS] on R_p and FTIR-RI of PANI copolymers

The [PDS] was varied between 1×10^{-2} and 3.5×10^{-2} M while keeping other experimental conditions constant. While increasing the [PDS] the R_p was increased abnormally. This is because of (1) production of more number of free radicals from PDS. (2) Auto acceleration effect due to formed copolymer surface. (3) Surface catalytic effect of nanomaterials. The order of reaction was determined by plotting log[PDS] vs. $\log R_p$ (Fig. 5a). The plot indicated a linear increasing trend with a slope value of 0.48 in the case of poly(ANI-co-OT)/clay. The same type of plot (Fig. 5b) was made for poly(ANI-co-OT)/TiO_2 system and the slope value was determined as 0.43. These values confirmed the 0.50 order of reaction with respect to [PDS] for both the copolymers. It means that 0.50 mol of PDS is required to initiate one mole of monomer in the presence of clay. In comparison, the clay system exhibited higher R_p values.

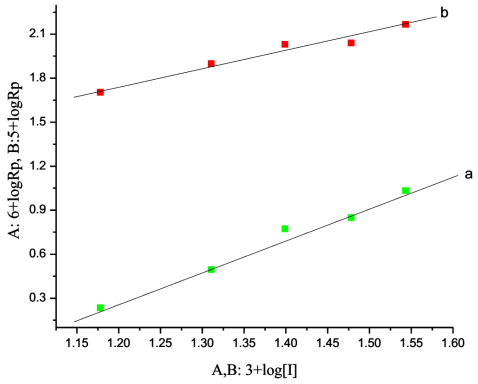

Fig. 5. Effect of [PDS] on R_p, (*a*) poly(ANI-co-OT)/clay system, (*b*) poly(ANI-co-OT)/TiO_2 system, [ANI] = 0.125 M, [OT] = 0.125 M, time = 2 h, temperature = 45 °C, wt% of nanomaterial = 3.

3.5. Effect of temperature on R_p and FTIR-RI of PANI copolymers

ANI and OT were copolymerized in the presence of clay under different temperatures. The temperature was varied between 273 and 343 K. During the temperature variation, the other experimental conditions were constant. While increasing the temperature the R_p value was increased. This is due to the following reasons. (1) Thermal initiation leads to formation of more and more monomer radical cations. (2) At higher temperature the dissociation rate of PDS was increased and hence production of more and more radicals. (3) Over oxidation or secondary oxidation led to the formation of oxidized quinonoid structure. (4) At higher temperature the clay moieties can swell more and more in the given reaction medium and the formation of monomer intercalated

structure which can be readily oxidized to form monomer radical cations. The energy of activation (E_a) for the formation of copolymer structure can be determined by the famous Arrhenius equation. The plot was made between $1/T$ and $\log R_p$ (Fig. 6a) to determine the E_a.

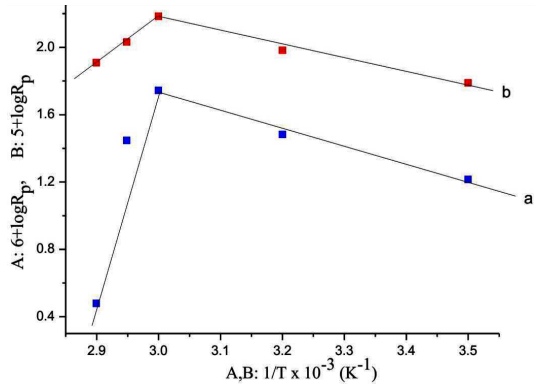

Fig. 6. Effect of temperature on R_p, (*a*) poly(ANI-co--OT)/TiO_2, (*b*) poly(ANI-co-OT) clay system, [ANI] = 0.125 M, [OT] = 0.125 M, time = 2 h, [PDS] = 0.025 M, wt% of nanomaterial = 3.

From the slope value of the above-mentioned plots, the E_a value was determined as 114.5 kJ/mol for ANI-OT--clay system. Similarly, in the copolymerization of ANI with TiO_2, the E_a value was determined as 108.6 kJ/mol (Fig. 6b). In comparison, the later system yielded lower E_a value and resulted with higher R_p values.

3.6. Effect of wt% of clay and TiO_2 on R_p and FTIR-RI of PANI copolymers

During the copolymerization of ANI with OT, the wt% of clay was varied from 1 to 5% by keeping the other experimental conditions as constant. While increasing the wt% of clay the R_p value was found to be increased. This is due to the following reasons. (1) At lower wt% loading of nanosized clay, there is a chance for the exfoliation of clay stacks by the monomers and more and more active surface area will be available for the initiation purpose. (2) Surface catalytic effect of nanosized clay can initiate the monomers [29]. (3) At higher wt% loading of clay, intercalation of more and more monomers into the basal spacing of clay stacks and results with monomer radical cations. In order to find out the order of polymerization reaction, Fig. 7a was made between log(wt% of clay) and $\log R_p$. The plot showed a straight line with a slope value of 0.48 which confirmed the 0.50 order of reaction with respect to wt% of clay. This inferred that 0.50 mol of clay is required to initiate one mole of monomer. In the case of poly(ANI-co-OT)/TiO_2 system, the slope value was calculated as 0.52 from the plot of log(wt% of TiO_2) vs. $\log R_p$ (Fig. 7b). Here also 0.50 mol of TiO_2 is required to initiate one mole of monomer. In comparison, the later system produced higher R_p values than the ANI--OT-clay system. This referred that R_p depends on the amount of the monomer used but also the structure of the nanomaterials used. The increase in R_p confirmed the role of nanomaterial as a catalyst through its surface effect. Currently, Anbarasan et al. [29] reported about the clay catalyzed synthesis of poly(α-naphthylamine), structurally similar to PANI, in which the R_p showed the first order reaction with respect to wt% of clay.

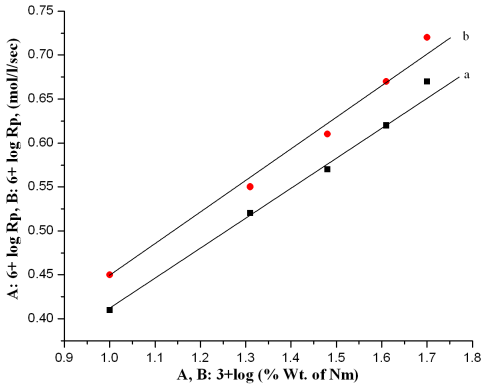

Fig. 7. (*a*) Effect of wt% of clay on R_p, (*b*) wt% of TiO_2 only, [ANI] = 0.125 M, [OT] = 0.125 M, time = 2 h, [PDS] = 0.025 M, temperature = 45 °C.

3.7. Thermogravimetric analysis

The TGA of 1 wt% clay loaded poly(ANI-co-OT)/clay (Fig. 8a) nanocomposite system showed a three-step degradation process. The first minor weight loss around 100 °C is due to the removal of moisture and physisorbed water molecules. The second minor weight loss is associated with the removal of chemisorbed water molecules and dopant from copolymer chain. The third major weight loss around 400 °C is due to the degradation of copolymer chain. Above 700 °C, it showed the residue of copolymer as 44.6% for 1 wt% of clay loaded copolymer and 58 wt% for 5 wt% of clay loaded copolymer, respectively. This indicated the improved thermal stability of copolymer nanocomposites.

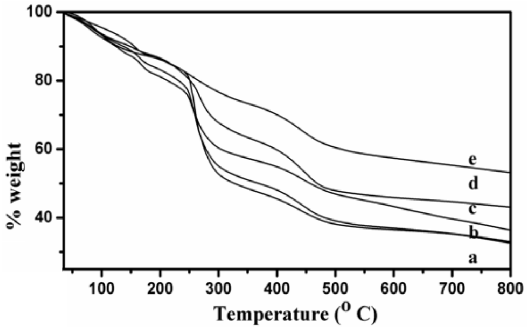

Fig. 8. TGA of poly(ANI-co-OT) loaded with clay at (*a*) 1 wt%, (*b*) 2 wt%, (*c*) 3 wt%, (*d*) 4 wt%, (*e*) 5 wt%.

Figure 8b–e explained the TGA of 2, 3, 4 and 5 wt% of clay loaded poly(ANI-co-OT). The thermogram of wt%

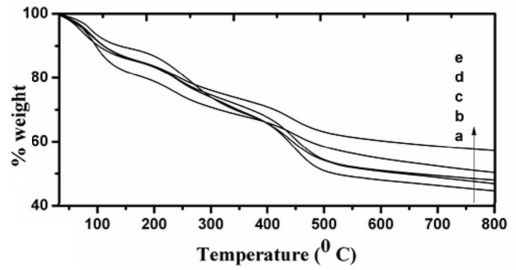

Fig. 9. TGA of poly(ANI-co-OT) loaded with TiO_2 (*a*) 1 wt%, (*b*) 2 wt%, (*c*) 3 wt%, (*d*) 4 wt%, (*e*) 5 wt%.

of TiO_2 loaded with the poly(ANI-co-OT)/TiO_2 showed the same type of degradation process. The wt% residue remaining above 700 °C was increased with the increase of wt% of TiO_2. TGA of 1 wt% of TiO_2 nanocomposite systems showed a three-step degradation process (Fig. 9). Above 700 °C the residue remaining is 42% for 1 wt% of TiO_2 and 60% for 5 wt% of TiO_2.

3.8. Conductivity measurements

Conductivity measurements informed that the co--monomer caused steric effect and hence reduction in conductivity value of a copolymer. The change in conductivity value is explained by altering the chemical structure of copolymer. Particularly, while increasing the wt% of nanomaterial, the conductivity value was increased slightly due to the host matrix nature of the nanomaterial. The electrical conductivity is increased due to the (1) higher % content of quinonoid form due to secondary oxidation, (2) increase of polymer chain length by surface catalytic effect due to the large surface area of nanomaterial, (3) doping nature of nanomaterials, (4) auto acceleration effect caused by polymeric surface, (5) charge mobility on the metal oxide surface [30].

The 1 and 5 wt% clay loaded copolymers exhibited the conductivity value of 5×10^{-4} and 6.8×10^{-4} S/cm, respectively, and that of TiO_2 loaded systems exhibited the conductivity value of 5.8×10^{-4} S/cm and 7.5×10^{-4} S/cm, respectively. Buvaneswari and co--workers [31] clearly explained the reasons for decrease in conductivity value of copolymer than the homopolymer.

3.9. HRTEM

Figure 10 represented the HRTEM of poly(ANI-co--OT)/clay nanocomposites. Figure 10a represented the layered structure of clay with the length of 5 to 10 nm with less than 0.1 nm breath. The same HRTEM image indicated the intercalation of copolymer chains into the basal spacing of clay. Figure 10b confirmed the agglomerated structure with the size of 20–25 nm. Figure 10c declared the bundle-like agglomerated structure due to the 5 wt% (heavy) loading of clay. Figure 10d revealed the linear agglomeration of clay particles with the size of 50–55 nm. The uniform dispersion of clay particles onto the matrix of copolymer was shown in Fig. 10e. The selected area electron diffraction pattern (SAED) (Fig. 10f) of copolymer nanocomposites showed some bright dots for (111), (200), (220) planes on a scattered manner. This indicates that the copolymer nanocomposites have a semicrystalline structure.

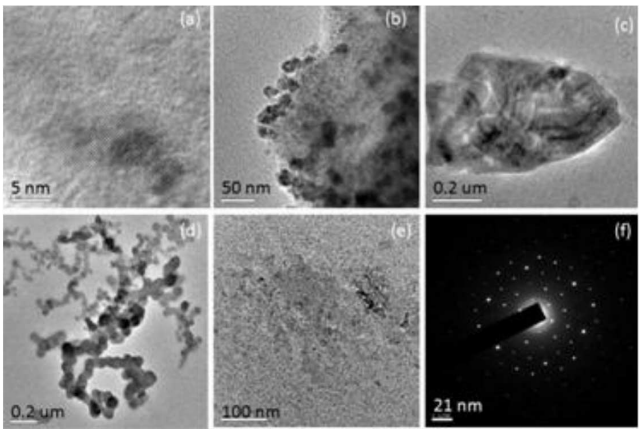

Fig. 10. HRTEM of poly(ANI-co-OT)-5 wt% clay polymer nanocomposite system.

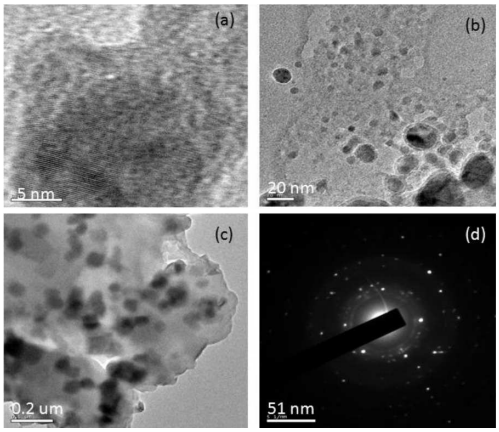

Fig. 11. HRTEM of poly(ANI-co-OT)-5 wt% TiO_2 polymer nanocomposite system.

Figure 11 indicated the HRTEM topography of poly(ANI-co-OT)/TiO_2 nanocomposite system. Figure 11a confirmed the layered structure [21] of TiO_2 with the length of 15–20 nm and with the breath of 0.1 nm. The dark area in the image confirmed the intercalation of copolymer into the interlayer space of TiO_2. The added TiO_2 uniformly distributed on the copolymer matrix without any agglomeration (Fig. 11b). Here the nanosized TiO_2 appeared as a distorted spherical morphology. Figure 11c revealed the distribution of agglomerated TiO_2 nanoparticle on the copolymer matrix. The agglomeration is due to the heavy loading of TiO_2. The agglomerated particles are having the size of 0.1 μm. The SAED pattern (Fig. 11d) exposed the bright spots

for (110), (101) planes in a random manner. This confirmed the less crystalline nature of poly(ANI-co-OT)/ TiO_2 nanocomposite system.

4. Conclusions

From the above kinetic study, the important points are presented here as conclusions. (1) The copolymer nanocomposites were synthesized by *in situ* oxidative polymerization method. (2) The structure of copolymer was altered by the clay and TiO_2 through its surface catalytic role. (3) The R_p and the FTIR-RI values were changed due to the change in the chemical structure of copolymer by the surface catalytic effect of clay and TiO_2. (4) The thermal stability of the copolymer was increased with the increase of wt% loading of clay and TiO_2 due to the intercalation of copolymer into the basal spacing of nanomaterial or exfoliation or delamination of nanomaterial stacks and dispersed on the copolymer matrix. (5) The conductivity value of the copolymer nanocomposite was increased as the wt% of nanomaterial increased.

References

[1] A. Vijayan, M. Fuke, M. Kulkarni, R.C. Iyer, *Sensors Actuat. B* **129**, 106 (2008).

[2] M.M. Ayad, N.A. Salahuddin, M.O. Alghaysh, *Polym. Adv. Tech.* **19**, 1142 (2008).

[3] G.C. Wang, Z.Y. Yang, X.W. Li, W.K. Yuan, *Mater. Res. Bull.* **43**, 214 (2008).

[4] C. Basavaraja, R. Pierson, D.S. Huh, *Eur. Polym. J.* **44**, 1556 (2008).

[5] Q. Chang, K. Zhao, X. Chen, M. Li, J.J. Liu, *J. Mater. Sci.* **43**, 5861 (2008).

[6] Y.T. Lim, J.H. Park, O.O. Park, *J. Colloid Inter. Sci.* **245**, 198 (2002).

[7] J. Dexmer, C.M. Leroy, L. Binet, C. Coulon, R. Backov, *Chem. Mater.* **20**, 5541 (2008).

[8] J. Jiang, *J. Macromol. Sci. Part B Phys.* **47**, 242 (2008).

[9] J. Jiang, L.H. Ai, *J. Macromol. Sci. Part B Phys.* **47**, 620 (2008).

[10] F. Wang, G. Wang, L. Du, H, C. Li, *J. Macromol. Sci. Part B Phys.* **47**, 743 (2008).

[11] S.F. Hameed, M.A. Allam, *J. Appl. Sci. Res.* **2**, 27 (2006).

[12] S. Chakraborty, S. Bandyopadhyay, R. Ameta, A.S. Deuri, *Polym. Test.* **26**, 38 (2007).

[13] F. Svegl, B. Orel, *Mat. Tech.* **37**, 29 (2003).

[14] J. Copikova, A. Synytsya, M. Novotna, *Czech J. Food Sci.* **19**, 51 (2001).

[15] J.S. Wang, J.S. Shi, Y.Z. Xu, X.Y. Duan, L. Zhang, J. Wang, L.M. Yang, S.F. Weng, J.G. Wu, *World J. Gastro.* **9**, 1897 (2003).

[16] A. Yelilarasi, J. Juliat Latha Jeyakumari, B. Sundaresan, V. Dhanalakshmi, R. Anbarasan, *Spectochim. Acta A* **74**, 1229 (2009).

[17] A. Yelilarasi, J. Juliat Latha Jeyakumari, B. Sundaresan, V. Dhanalakshmi, R. Anbarasan, *Polym. Comp.* **17**, 397 (2009).

[18] M. Fathima Parveen, S. Umapathy, V. Dhanlakshmi, R. Anbarasan, *Nano* **4**, 147 (2009).

[19] M. Fathima Parveen, S. Umapathy, V. Dhanlakshmi, R. Anbarasan, *J. Mater. Sci.* **44**, 5852 (2009).

[20] V. Parthasarathy, B. Sundaresan, V. Dhanalakshmi, R. Anbarasan, *Polym. Eng. Sci.* **20**, 474 (2010).

[21] S. Xiong, Q. Wang, Y. Chen, *J. Appl. Polym. Sci.* **111**, 963 (2009).

[22] S. Sedaghat, F. Golbaz, *J. Nanostruct. Chem.* **3**, 65 (2013).

[23] N. Vijayakumar, E. Subramanian, D. Pathinettam, Padiyan, *Polym. Plast. Tech. Eng.* **52**, 1175 (2013).

[24] R. Anbarasan, S.A. Anton Kumanan, R. Siva, V. Dhanalakshmi, *Int. J. Pure Appl. Chem.* **4**, 47 (2009).

[25] R. Anbarasan, S. Kanchana, S. Gayathri, T. Jayalakshmi, V. Dhanalakshmi, *J. Appl. Polym. Sci.* **115**, 315 (2010).

[26] R. Anbarasan, K. Rajasulochana, M. Sudha, M. Anusuya, T. Jayalakshmi, V. Dhanalakshmi, *J. Appl. Polym. Sci.* **115**, 2582 (2010).

[27] R. Anbarasan, O. Babout, M. Dequiel, B. Maillard, *J. Appl. Polym. Sci.* **97**, 761 (2005).

[28] R. Anbarasan, O. Babout, M. Dequiel, B. Maillard, *J. Appl. Polym. Sci.* **97**, 766 (2005).

[29] R. Anbarasan, S. Sivakumaravel, C. Gopiganesh, *Int. J. Polym. Mater.* **55**, 803 (2006).

[30] A. Yelilarasi, J. Juliet Latha Jeyakumari, B. Sundaresan, V. Dhanalakshmi, R. Anbarasan, *J. Chil. Chem. Soc.* **56**, 610 (2011).

[31] R. Buvaneswari, A. Gopalan, T. Vasudevan, *Thin Solid Films* **458**, 77 (2004).